LINEAR BEHAVIOR OF SHALLOW TRANSLATIONAL SHELLS WITH CLAMPED SUPPORT ALONG EDGES

Youichi MINAKAWA

(Received May 31, 1984)

Summary

In previous analyses of shallow translational shells, not much consideration was given to the inplane displacement. But, analyses of shells with pinned and roller supports along the edges made clear that the boundary conditions have considerable effects on the behavior of the shells. Here, shells with clamped supports are analyzed and effects of curvatures on their behavior are examined.

1. Introduction

The static behavior of shallow translational shells are usually understood by applying a generalized Levy-type solution to the Marguerre-Vlasov equation.[1,2,7] To simplify calculations Poisson's ratio is almost always neglected. The generalized Levy-type solution is not suitable to solve natural frequencies of the shells, because the characteristic equations to get homogeneous solutions for the generalized Levy-type solution have coefficients with unknown natural frequency.[4,5]

On the other hand, the natural frequencies of the shells can be determined by adopting the Galerkin method.[6,8,9] However, in the analyses, the boundary condition for inplane displacements along edges do not recieve due consideration.

Minakawa et al[10] analyzed shells with pinned support and showed that Poisson's ratio have considarable effects on the behavior of the shallow shells. In this paper shallow shells are analyzed under clamped supports and Poisson's ratio and the curvature effects on linear behavior of the shells are examined.

2. Basic Equations for Shallow Translational Shells

The mid-surface of the translational shallow shells examined here is given by

$$z(x, y)=\frac{1}{2}\left\{\frac{x(x-a)}{R_x}+\frac{y(y-b)}{R_y}\right\} \tag{1}$$

where x, y, z are the cartesian cordinates, and R_x and R_y are constants identifying the radii of curvature in the x and y direction, respectively. The shells have a rectangular planform of dimensions $a\times b$ with boundaries along $x=0$, a and $y=0$, b illustrated in Fig. 1. Without tangential inertia force, linear equation for the shells in terms of the normal displacement w and the Airy's stress function Φ are expressed by

$$L(w, \Phi)=D\nabla^2\nabla^2 w+\frac{1}{R_x}\frac{\partial^2\Phi}{\partial y^2}+\frac{1}{R_y}\frac{\partial^2\Phi}{\partial x^2}+\rho h\frac{\partial^2 w}{\partial t^2}-p=0 \tag{2-a}$$

$$\frac{1}{Eh}\nabla^2\nabla^2\Phi-\frac{1}{R_x}\frac{\partial^2 w}{\partial y^2}-\frac{1}{R_y}\frac{\partial^2 w}{\partial x^2}=0 \tag{2-b}$$

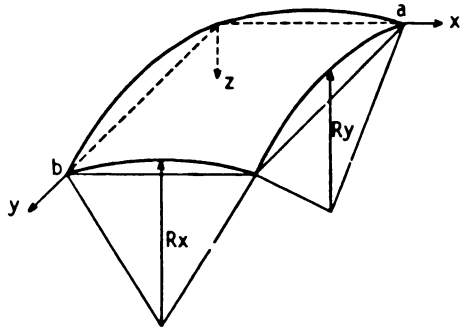

Fig. 1 Geometry of Shells

where h= shell thickness, E= Young's modulus, ρ= mass density, ν= Poisson's ratio, p= normal pressure load and $D=Eh^3/12(1-\nu^2)$.

The membrane stress resultants N_x, N_y, N_{xy}, the bending and twisting moments M_x, M_y, M_{xy}, and the inplane displacement components u and v corresponding to x and y direction, respectively, are given by

$$N_x=\frac{\partial^2\Phi}{\partial y^2},\quad N_y=\frac{\partial^2\Phi}{\partial x^2},\quad N_{xy}=-\frac{\partial^2\Phi}{\partial x\partial y} \tag{3-a}$$

$$M_x=-D\left(\frac{\partial^2 w}{\partial x^2}+\nu\frac{\partial^2 w}{\partial y^2}\right),\quad M_y=-D\left(\frac{\partial^2 w}{\partial y^2}+\nu\frac{\partial^2 w}{\partial x^2}\right),\quad M_{xy}=D(1-\nu)\frac{\partial^2 w}{\partial x\partial y} \tag{3-b}$$

$$u=\int\left\{\frac{1}{Eh}\left(\frac{\partial^2\Phi}{\partial y^2}-\nu\frac{\partial^2\Phi}{\partial x^2}\right)+\frac{w}{R_x}\right\}dx,\quad v=\int\left\{\frac{1}{Eh}\left(\frac{\partial^2\Phi}{\partial x^2}-\nu\frac{\partial^2\Phi}{\partial y^2}\right)+\frac{w}{R_y}\right\}dy \tag{3-c}$$

The shallow shells are solved under the boundary condition with clamped support along edges expressed by

$$w=\frac{\partial w}{\partial x}=0,\ \text{and}\ u=v=0\ \text{at}\ x=0\ \text{and}\ a \tag{4-a,b}$$

$$w=\frac{\partial w}{\partial y}=0,\ \text{and}\ u=v=0\ \text{at}\ y=0\ \text{and}\ b \tag{4-c,d}$$

3. Analyzing procedure

The normal displacement w under the conditions given by Eqs. (4-a, c) is assumed by

$$w(x,y)=\sum_m\sum_n w_{mn}(\cos\alpha_m x-1)(\cos\beta_n y-1)\quad (m,\ n=2,\ 4,\ 6\cdots) \tag{5}$$

where $\alpha_m=m\pi/a$, $\beta_n=n\pi/b$. In order to simplify the analysis, we restrict the case where the normal displacement is symmetric with respect to $x=a/2$ and $y=b/2$, i. e. integers m and n take even numbers. Substituting Eq. (5) into Eq. (2-b), we have a particular solution Φ_p for stress function

$$\Phi_p(x,y)=\frac{Eha^2}{R_x}\sum_m\sum_n\frac{w_{mn}}{\pi^2}\left\{\frac{(\lambda m^2+\gamma^2 n^2)}{(m^2+\gamma^2 n^2)^2}\cos\alpha_m x\cos\beta_n y-\frac{\lambda}{m^2}\cos\alpha_m x-\frac{1}{\gamma^2 n^2}\cos\beta_n y\right\} \tag{6}$$

where $\gamma=a/b$, and $\lambda=R_x/R_y$. The homogeneous solution Φ_h for the stress function is assumed by

$$\Phi_h(x,y)=\frac{Eha^2}{R_x}\left[\sum_m\left\{A_1{}^m\cosh\alpha_m\left(y-\frac{b}{2}\right)+A_3{}^m\alpha_m\left(y-\frac{b}{2}\right)\sinh\alpha_m\left(y-\frac{b}{2}\right)\right\}\cos\alpha_m x\right.$$

$$+\sum_n\left\{B_1^n\cosh\beta_n\left(x-\frac{a}{2}\right)+B_3^n\beta_n\left(x-\frac{a}{2}\right)\sinh\left(x-\frac{a}{2}\right)\right\}\cos\beta_n y+\frac{C_1}{2a^2}\left(x-\frac{a}{2}\right)^2+\frac{C_2}{2a^2}\left(y-\frac{b}{2}\right)^2\Big] \quad (7\text{-a})$$

where the polynomial terms are included. The reason why the polynomial terms are added to the stress function is shown in following description. Substituting the general solution for the stress function and w in Ep.(**3-c, d**), we may have $u(x, y)$ and $v(x, y)$.

$$u(x,y)=\frac{a}{R_x}\Big[\sum_m m\pi\Big[\{(1+\nu)A_1^m+2A_3^m\}\cosh\alpha_m\left(y-\frac{b}{2}\right)+A_3^m\alpha_m(1+\nu)\left(y-\frac{b}{2}\right)\sinh\alpha_m\left(y-\frac{b}{2}\right)\Big]\sin\alpha_m x$$
$$-\sum_n\gamma n\pi\Big[\{B_1^n(1+\nu)+B_3^n(\nu-1)\}\sinh\beta_n\left(x-\frac{a}{2}\right)+B_3^n(1+\nu)\beta_n\left(x-\frac{a}{2}\right)\cosh\beta_n\left(x-\frac{a}{2}\right)\Big]\cos\beta_n y$$
$$+\frac{C_2-\nu C_1}{a}\left(x-\frac{a}{2}\right)+\sum_m\sum_n\frac{w_{mn}}{m\pi}\Big[-\frac{\lambda m^2+\gamma^2n^2}{(m^2+\gamma^2n^2)^2}(\gamma^2n^2-\nu m^2)\sin\alpha_m x\cos\beta_n y+\alpha_m\left(x-\frac{a}{2}\right)\cos\beta_n y$$
$$-\nu\lambda\sin\alpha_m x+\left\{\sin\alpha_m x-\alpha_m\left(x-\frac{a}{2}\right)\right\}(\cos\beta_n y-1)\Big]\Big] \quad (8\text{-a})$$

$$v(x,y)=\frac{a}{R_x}\Big[-\sum_m m\pi\Big[\{A_1^m(1+\nu)+A_3^m(\nu-1)\}\sinh\alpha_m\left(y-\frac{b}{2}\right)+A_3^m(1+\nu)\alpha_m\left(y-\frac{b}{2}\right)\cosh\alpha_m\left(y-\frac{b}{2}\right)\Big]$$
$$\times\cos\alpha_m x+\sum_n\gamma n\pi\Big[\{B_1^n(1+\nu)+2B_3^n\}\cosh\beta_n\left(x-\frac{a}{2}\right)+B_3^n(1+\nu)\beta_n\left(x-\frac{a}{2}\right)\sinh\beta_n\left(x-\frac{a}{2}\right)\Big]\sin\beta_n y$$
$$+\frac{C_1-\nu C_2}{a}\left(y-\frac{b}{2}\right)+\sum_m\sum_n\frac{w_{mn}}{\gamma n\pi}\Big[-\frac{\lambda m^2+\gamma^2n^2}{(m^2+\gamma^2n^2)^2}(m^2-\nu\gamma^2n^2)\cos\alpha_m x\sin\beta_n y-\nu\sin\beta_n y$$
$$+\lambda\beta_n\left(y-\frac{b}{2}\right)\cos\alpha_m x+\lambda\left\{\sin\beta_n y-\beta_n\left(y-\frac{b}{2}\right)\right\}(\cos\alpha_m x-1)\Big]\Big] \quad (8\text{-b})$$

At the boundary $x=0$ and $y=0$, we have

$$u(x,0)=\frac{a}{R_x}\Big[\sum_m m\pi\Big[\{A_1^m(1+\nu)+2A_3^m\}\cosh\frac{m\pi}{2\gamma}+A_3^m(1+\nu)\frac{m\pi}{2\gamma}\sinh\frac{m\pi}{2\gamma}\Big]\sinh\alpha_m x$$
$$-\sum_n\gamma n\pi\Big[\{B_1^n(1+\nu)+B_3^n(\nu-1)\}\sinh\beta_n\left(x-\frac{a}{2}\right)+B_3^n(1+\nu)\beta_n\left(x-\frac{a}{2}\right)\cosh\beta_n\left(x-\frac{a}{2}\right)\Big]$$
$$+\frac{C_2-\nu C_1}{a}\left(x-\frac{a}{2}\right)+\sum_m\sum_n\frac{w_{mn}}{m\pi}\Big[-\frac{\lambda m^2+\gamma^2n^2}{(m^2+\gamma^2n^2)^2}(\gamma^2n^2-\nu m^2)\sin\alpha_m x+\alpha_m\left(x-\frac{a}{2}\right)-\nu\lambda\sin\alpha_m x\Big]\Big] \quad (9\text{-a})$$

$$v(0,y)=\frac{a}{R_x}\Big[-\sum_m m\pi\Big[\{A_1^m(1+\nu)+A_3^m(\nu-1)\}\sinh\alpha_m\left(y-\frac{b}{2}\right)+A_3^m(1+\nu)\alpha_m\left(y-\frac{b}{2}\right)\cosh\alpha_m\left(y-\frac{b}{2}\right)\Big]$$
$$+\sum_n\gamma n\pi\Big[\{B_1^n(1+\nu)+2B_3^n\}\cosh\frac{\gamma n\pi}{2}+B_3^n(1+\nu)\frac{\gamma n\pi}{2}\sinh\frac{\gamma n\pi}{2}\Big]\sin\beta_n y+\frac{C_2-\nu C_1}{a}\left(y-\frac{b}{2}\right)$$
$$+\sum_m\sum_n\frac{w_{mn}}{m\pi}\Big[-\frac{\lambda m^2+\gamma^2n^2}{(m^2+\gamma^2n^2)^2}(m^2-\nu\gamma^2n^2)\sin\beta_n y-\nu\sin\beta_n y+\lambda\beta_n\left(y-\frac{b}{2}\right)\Big]\Big] \quad (9\text{-b})$$

$$u(0,y)=\frac{a}{R_x}\Big[\sum_n\gamma n\pi\Big[\{B_1^n(1+\nu)+B_3^n(\nu-1)\}\sinh\frac{\gamma n\pi}{2}+B_3^n(1+\nu)\frac{\gamma n\pi}{2}\cosh\frac{\gamma n\pi}{2}\Big]\cos\beta_n y$$
$$-\frac{C_2-\nu C_1}{2}-\sum_m\sum_n\frac{w_{mn}}{2}\Big] \quad (9\text{-c})$$

$$v(x,0)=\frac{a}{R_x}\Big[\sum_m m\pi\Big[\{A_1^m(1+\nu)+A_3^m(\nu-1)\}\sinh\frac{m\pi}{2\gamma}+A_3^m(1+\nu)\frac{m\pi}{2\gamma}\cosh\frac{m\pi}{2\gamma}\Big]\cos\alpha_m x$$
$$-\frac{C_1-\nu C_2}{2\gamma}-\sum_m\sum_n\frac{w_{mn}}{2}\Big] \quad (9\text{-d})$$

When Eq.(**9-a**) is expanded in Fourier Sine series, the following condition guarantees uniform convergence in closed interval $[0, a]$

$$u(0,0)=u(a,0)=-(C_2-\nu C_1+\sum_m\sum_n w_{mn})/2=0 \quad (10\text{-a})$$

The requirement also coincides with the condition that the constant component for Fourier Cosine series of Eq. (9 -c) is vanished. Similarly, requirement for Eqs. (9 -b, d) is given by

$$v(0\ ,\ 0)=v(0\ ,\ b)=-(C_1-\nu C_2+\lambda\sum_m\sum_n w_{mn})/2=0 \qquad (10\text{-b})$$

Substituting Eq. (10) into Eqs. (9 -c, d), the boundary conditions for $u(0\ ,\ y)=v(x\ ,\ 0)=0$ are expressed by

$$\{B_1^n(1+\nu)+B_3^n(\nu-1)\}\sinh\frac{\gamma n\pi}{2}+B_3^n(1+\nu)\frac{\gamma n\pi}{2}\cosh\frac{\gamma n\pi}{2}=0 \quad \text{for each } n \qquad (11\text{-a})$$

$$\{A_1^m(1+\nu)+A_3^m(\nu-1)\}\sinh\frac{m\pi}{2\gamma}+A_3^m(1+\nu)\frac{m\pi}{2\gamma}\cosh\frac{m\pi}{2\gamma}=0 \quad \text{for each } m \qquad (11\text{-b})$$

Under the conditions in Eqs. (10-a, b), Eqs. (9 -a, b) are expanded into the following

$$u(x\ ,\ 0)=\frac{a}{R_x}\sum_m\tilde{u}_m\sin\alpha_m x \qquad (12\text{-a})$$

$$v(0\ ,\ y)=\frac{a}{R_x}\sum_n\tilde{v}_n\sin\beta_n y \qquad (12\text{-b})$$

The boundary conditions $u(x\ ,\ 0)=v(0\ ,\ y)=0$ give

$\tilde{u}_m=0$ for each m ($m=2,\ 4,\ 6\ \cdots\cdots$) (13-a)

$\tilde{v}_n=0$ for each n ($n=2,\ 4,\ 6\ \cdots\cdots$) (13-b)

Setting the numbers $m,\ n=2,4,6,\cdots,\ 2N$, we can express Eqs. (11-a, b) and Eqs. (13-a, b) in matrix form

$$[S]\{c\}=[F]\{d\} \qquad (14)$$

where $\{c\}=\{A_1^2A_3^2B_1^2B_3^2\cdots A_1^{2N}A_3^{2N}B_1^{2N}B_3^{2N}\}$, $\{d\}=\{w_{22}w_{24}w_{42}\cdots w_{2N2N}\}$.

The expression guarantees the inplane constraint along edges. Then, applying the Galerkin method to Eq. (2 -b), we have

$$\frac{R_x^2}{Eh}\frac{4}{ab}\int_0^a\int_0^b L(w\ ,\ \Phi)(\cos\alpha_{\tilde{m}}-1)(\cos\beta_{\tilde{n}}-1)dxdy=0 \quad \text{for each } \tilde{m},\ \tilde{n} \qquad (15)$$

where $\tilde{m},\ \tilde{n}=2,\ 4,\ 6\cdots,\ 2N$. Expressing Eq. (15) in matrix form, we have

$$\frac{\rho R_x^2}{E}[M]\{\ddot{d}\}+[G_1\ G_2]\begin{Bmatrix}d\\c\end{Bmatrix}=\{P\}. \qquad (16)$$

where dot denotes differential with respect t. Substituting Eq. (14) into Eq. (16), we get the ordinary differentical equation of motion

$$\frac{\rho R_x^2}{E}[M]\{\ddot{d}\}+[K]\{d\}=\{P\} \qquad (17)$$

where $[K]=[G_1]+[G_2][S]^{-1}[F]$. When Eq. (2) is solved under the boundary condition given by Eqs. (4), the mass matrix $[M]$ and the stiffness matrix $[K]$ are both symmetric matrices.

Set $\{d\}=\{\phi\}\exp(i\omega t)$, we have the eigenvalue problem for natural frequencies

$$\omega^2\frac{\rho R_x^2}{E}[M]\{\phi\}=[K]\{\phi\} \qquad (18)$$

Since each component of matrices $[M]$ and $[K]$ is expressed in nondimensional parameters $\lambda(=R_x/R_y)$, $\mu(=a^2/R_xh)$, $\gamma(=a/b)$ and Poisson's ratio ν, natural frequency ω is expressed in nondimensional natural frequency factor given by

$$\Omega=\omega\sqrt{\frac{E}{\rho R_x^2}} \qquad (19)$$

4. Numerical results

4 − 1 Static analyses

Setting N=3, 4, ···, 11 for the shell with $\gamma=1$, $\lambda=0$, $\mu=50$, $\nu=0$ under the uniform hydro-pressure load, we examine the convergence of normal displacement w and bending moment Mx, and show the results in Fig. 2 where the displacement w_c and the bending moment Mc at the middle point presented in the form

$$w(a/2\ ,\ b/2)=w_c\times pa^4/Eh^3,\quad Mx(a/2\ ,\ b/2)=Mc\times pa^2$$

Then, setting $\nu=0$ and $\nu=0.3$ for the shell with $\gamma=1$, $\mu=50$ and adopting N=10, we calculate w_c and the mean value factor $\overline{w}$ given by

$$\frac{1}{ab}\int_0^a\int_0^b w(x\ ,\ y)dxdy=\overline{w}\times pa^4/Eh^3$$

and illustrate $\overline{w}-\lambda$ curves with solids lines and $w_c-\lambda$ curves with broken lines in Fig. 3. It is interesting results that normal displacement at the middle point for the shell with clamped support is larger than the displacement for the shell with pinned support.[10] However, the mean value for the displacement of the former shells smaller than the value of the latter shells, which is a natural consequence.

When $\nu=0$, though w_c and $\overline{w}$ for the shell with positive Gaussian curvature λ are a little smaller than those for the shell with negative Gaussian curvature $-\lambda$, w_c and $\overline{w}$ for the shells with same absolute value $|\lambda|$ are almost the same. When the Poisson's ratio changes from 0 to 0.3, while the other parameters are unchanged, the shells with λ behave like the shells having about 0.16~0.20 larger Gaussian curvature.

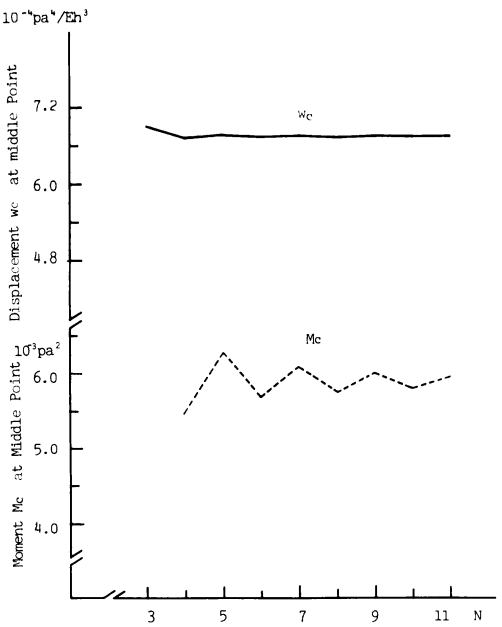

Fig. 2 Convergences of w_c and Mc with respect to N

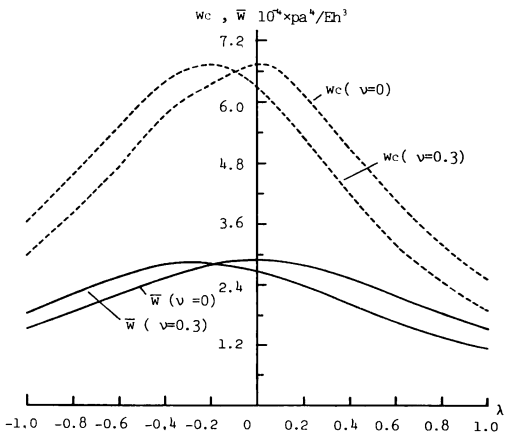

Fig. 3 w_c vs λ and w vs λ Curves

Because the characteristic equations include Poisson's ratio and derivations require troublesome calculation, many papers neglect the ratio. Here, in order to examine the ratio to displacement distributions of the shell analyzed by Nakata et al,[2] we solve the shell with $\gamma=1$, $\mu=150$, $\lambda=1$, $\nu=0$ and $\nu=0.3$ and illustrated in Fig. 4.

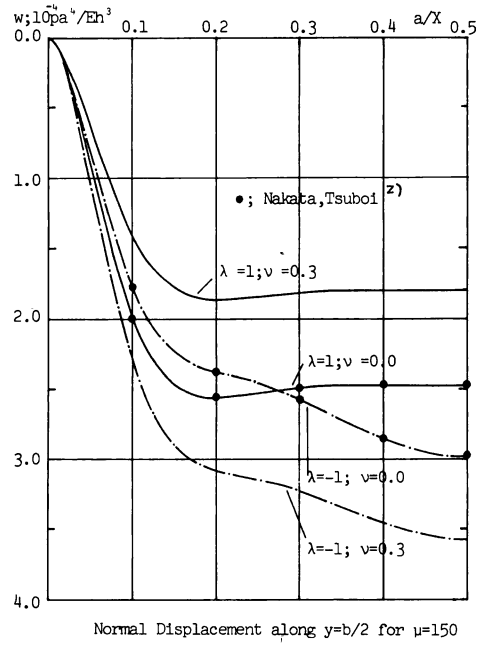

Fig. 4 Displacement Distribution ($\gamma=1$, $\mu=150$)

4 − 2 Natural frequency analyses

The eigenvalues obtained from the eivenvalue problem in Eq. (18) are numbered by

$$\omega_1<\omega_2<\omega_3<\cdots \tag{20}$$

and the eigenvector corresponding to ω_i is normalized with respect to the mass matrix

$$\{\phi_i\}^T[M]\{\phi_i\}=1 \tag{21}$$

Setting N=1, 2, ···, 9 for the shell with $\gamma=1$, $\lambda=-1$, $\mu=160$, $\nu=0.3$, we examine the convergence of natural frequencies and illustrate in Fig. 5.

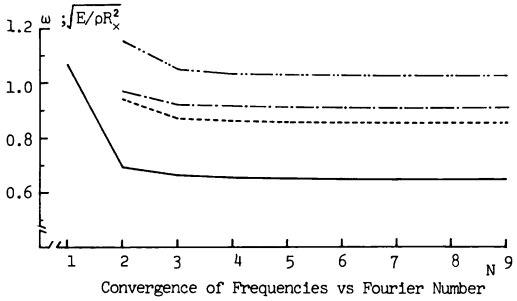

Fig. 5 Convergences of Natural Frequencies ($\gamma=1$, $\mu=160$, $\lambda=-1$, $\nu=0.3$)

For the shell with $\lambda=1$, $\mu=50$, $\lambda=0$, the variation of ω_i with λ ($i=1, \cdots, 4$) are depicted in Fig. 6. The solid lines correspond to the eigenvectors where w_{22} takes the maximum. Since the eigenfunctions corresponding to eigenvalues vary with respect to λ, the solid lines observed on different eigenvalue curves.

In order to examine effects of Poisson's ratio on natural frequencies, we analyze the shell with $\nu=0.3$, $\gamma=1$, $\mu=50$ and the shell with $\nu=0$, $\gamma=1$, $\mu=50$, and illustrate each ratio of the former frequency $\omega_i|_{\nu=0.3}$ and the latter one $\omega_i|_{\nu=0}$ with λ, denoted $\omega_{0.3}/\omega_0-\lambda$ curves in Fig. 7. For every frequency for plates, the ratio becomes $(1-\nu^2)^{-1/2}|_{\nu=0.3}=1.0483$. Judging from Figs. 6 and 7, it is found that each natural frequency on which Poisson's ratio has a considerable influence may correspond to the eigenvector where w_{22} takes the maximum. Therefore, we may say that the in-

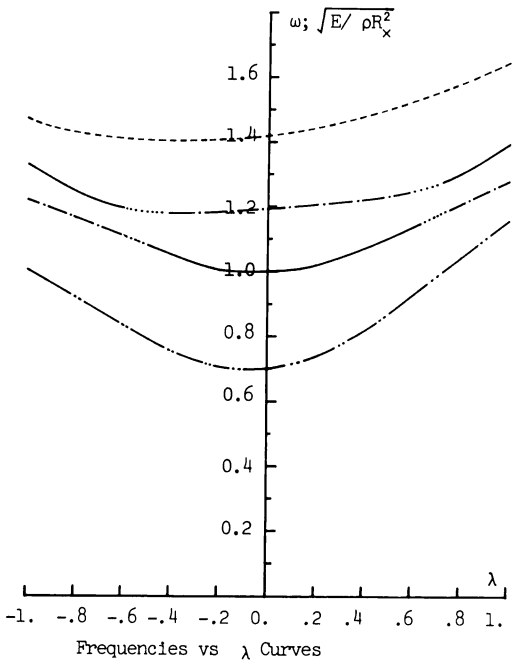

Fig. 6 Frequencies vs λ curves ($\gamma=1$, $\mu=50$, $\nu=0$)

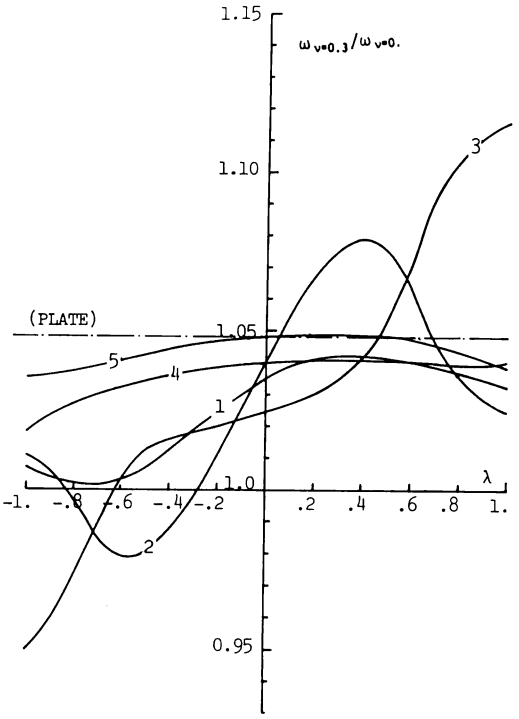

Fig. 7 $\omega_{0.3}/\omega_0$ vs λ curves ($\gamma=1$, $\mu=50$, $\nu=0$)

crease of Poisson's ratio lets increase the natural frequency corresponding to the eigenfunction with the maximum volume change for the shells in the region $\lambda>0$, especially for the shells in the neighborhood region $\gamma=1$, and lets decrease the natural frequency for the shells in the region $\lambda<0$, especially for the shell in the neighborfood $\gamma=-1$.

Then, we seek the membrane energy for each eigenvector normalized in Eq. (21). The membrane energy factor U is defined by

$$\frac{1}{2}\int_0^a\int_0^b \frac{1}{Eh}\{N_x^2+N_y^2-2\nu N_xN_y+2(1+\nu)N_{xy}^2\}\,dxdy=U\times\frac{Eh^3}{a^2}$$

Setting $\gamma=1$, $\mu=50$, $\nu=0$, the energy factor for each eigenvector corresponding to the eigenvalue ω_i is illustrated in Fig. 8.

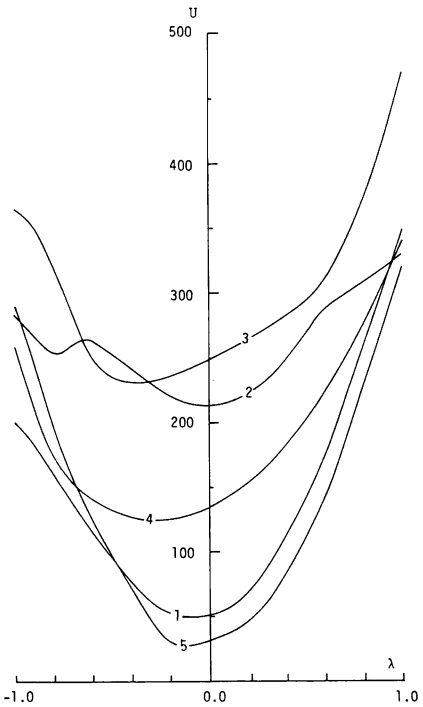

Fig. 8 Membrane enrgy U vs λ curves ($\gamma=1$, $\mu=50$, $\nu=0$)

Conclusion

Linear Bahaviors of shallow shell with clamped support along edges are studied. The results of static analyses under uniform hydropressure load are summarized as follows

1. When Poisson's ratio is zero, the whole normal displacement of the shell with $\lambda>0$ is a little smaller than that of the shell with $\lambda<0$, where the shells with the same absolute value $|\lambda|$ are compared. But, there are not significant differences between them.

2. The increase of Poisson's ratio make decrease the displacement of shells with $\lambda>0$ and make increase that with $\lambda<0$.

3. For shells with μ being larger than a certain value, the normal displacement at the middle point for the shell with clamped support is larger than the displacemtnt for the shell with pinned support, which is interesting results.

The results of natural frequency analyses are summarized as follows

4. The effects of changing Poisson's ratio on natural frequency of the shells corresponding to eigenvector with more membrane energy differ from the effects on natural frequency of plates.

5. The increase of Poisson's ratio makes increase the natural frequency corresponding to eigenfunction with more membrane energy for the shell in neighborhood region $\gamma=1$, but makes decrease the natural frequency corresponding to it with the shell in the neighborhood region $\gamma=-1$.

References

1) 坪井，高橋 “周辺固定支持されたH. P. シェルのフーリェ解析” 日本建築学会論文報告集第104号昭和39年

2) 中田，坪井“偏平ＨＰおよびＥＰシェルのフーリェ弾性解析”
日本建築学会論文報告集第318号昭和57年
3) 清水，真瀬，伊藤，和泉“偏平推動殻の応力分布へ及ぼす曲率の影響”建築学会東北支部昭和52年
4) 横尾，国枝“偏平シェルの振動(Ⅰ)”及び(Ⅱ)
日本建築学会論文報告集第114号昭和40年
5) H. Kunieda “Solution of Free Vibrations of Spherical Shells”
日本建築学会論文報告集第325号昭和58年
6) E. Reissner “On Transverse Vibrations of Thin Shallow Elastic Shell” Q. Appl. Math. 13, 1955
7) K. Apeland “Stress Analysis of Translational Shells” A. S. C. E. EMI, p. 2743, 1961
8) A. W. Leissa and A. S. Kadi “Curvature Effects on Shallow Shell Vibrations” J. Sound Vib. 16, p. 173, 1971
9) K. Kanazawa and Y. Hangai “Nonlinear Flexural Vibration of Thin Shallow Shells” Proc. 25 th Japan National Congress for Applied Mechanics, 1975
10) Y. Minakawa, T. Uchiyama and T. Norimatsu “Linear Behaviors of Shallow Translational Shells with Pinned Support along Edges” 鹿児島大学工学部研究報告第25号昭和58年
11) 皆川“周辺固定の偏平推動殻の線形解析”
日本建築学会大会昭和58年
12) 坪井善勝“連続体力学序説”産業図書